Genomics Data 6 (2015) 40–43

Contents lists available at ScienceDirect

Genomics Data

journal homepage: http://www.journals.elsevier.com/genomics-data/

Data in Brief

Transcriptional profiling of radiation damage and preventive treatments in a 3-dimensional (3D) human cell culture model of oral mucositis

Maria P. Lambros [a,*], Michael K. DeSalvo [b], Jonathan Moreno [a], Hari Chandana Mulamalla [a], Lavanya Kondapalli [a]

[a] College of Pharmacy, Western University of Health Sciences, Pomona, CA 91766, USA
[b] Gran, LLC, Fullerton, CA 92835, USA

ARTICLE INFO

Article history:
Received 26 July 2015
Accepted 31 July 2015
Available online 4 August 2015

ABSTRACT

Cancer patients who receive radiation are often afflicted by oral mucositis, a debilitating disease, characterized by mouth sores and difficulty in swallowing. Oftentimes, cancer patients afflicted with mucositis must stop life-saving therapies. Thus it is very important to prevent mucositis before it develops. Using a validated organotypic model of human oral mucosa, a 3-dimensional cell culture model of human oral keratinocytes, it has been shown that a mixture (NAC–QYD) of N-acetyl cysteine (NAC) and a traditional Chinese medicine, Qingre Liyan decoction (QYD), prevented radiation damage (Lambros et al., 2014). Here we provide detailed methods and analysis of microarray data for non-irradiated and irradiated human oral mucosal tissue with and without pretreatment with NAC, QYD and NAC-QYD. The microarray data been deposited in Gene Expression Omnibus (GEO): GSE62397. These data can be used to further elucidate the mechanisms of irradiation damage in oral mucosa and its prevention.

Specifications	
Organism/cell line/tissue	Human primary oral keratinocytes grown in 3D culture
Sex	Male
Sequencer or array type	Phalanx Human OneArray v5 (GPL13693)
Data format	Raw and processed
Experimental factors	Control (non-pretreated, non-irradiated) compared to: (1) non-pretreated, irradiated; (2) pretreated with NAC, irradiated; (3) pretreated with QYD, irradiated; (4) pretreated with NAC- QYD, irradiated.
Experimental features	3D oral tissues were exposed to gamma irradiation exposure at 12 Gy. After irradiation, the tissues were incubated for 6 h at 37 °C with 5% CO_2. Subsequently, some of the tissues were used for the extraction of total RNA, and others were placed in 10% formalin for histopathological studies. For pretreated samples, the apical surface of the 3D tissues was exposed to 100 μL of NAC, QYD, or NAC–QYD. The tissues were then rinsed with phosphate-buffered saline to remove the treatment materials and transferred to new plates with fresh culture medium.
Consent	N/A
Sample source location	Pomona, CA

1. Direct link to deposited data

http://www.ncbi.nlm.nih.gov/geo/query/acc.cgi?acc=GSE62397

2. Experimental design, materials and methods

2.1. Tissue culture and irradiation

All tissue culture and irradiation methods are previously described [1]. The 3D human primary cell culture of oral keratinocytes (tissues) and media (containing specially prepared phenol red, 5 μg/mL gentamicin, and 0.25 μg/mL amphotericin B) were purchased from MatTek Corporation (Ashland, MA). The oral (buccal) keratinocytes were grown in Millipore Millicell tissue-culture plate inserts in serum-free media at 37 °C with 5% CO_2. The resultant 3D cultures showed high degree of differentiation and were similar to buccal epithelial. The 3D tissues were incubated with 100 μL of one of the following mixtures for 2 h at 37 °C: (a) 1 mM NAC, (b) 5 mg/mL QYD, or (c) an NAC–QYD mixture consisting of 1 mM NAC and 4.5 mg/mL QYD. After the incubation, the tissues were rinsed with phosphate-buffered saline, placed in new plates with fresh media and irradiated with 12 Gy. The irradiation took place at the facilities of City of Hope, Duarte, CA. At least three 3D oral tissues were used for each treatment. Two or more tissues were used for extraction of total RNA.

2.2. RNA isolation and microarray hybridization

Total RNA was extracted using the RNeasy Plus Mini Kit (Qiagen, Germantown, MD). RNA of at least 2 identically treated 3D tissues was combined and used for analysis. Using an Agilent 2100 Bioanalyzer (Agilent Technologies, Palo Alto, CA), and by evaluating the A260/280

* Corresponding author.

http://dx.doi.org/10.1016/j.gdata.2015.07.029

absorbance ratio, the integrity and quality of RNA was determined. Only RNA with absorbance ratio, A260/280 > 1.9, and RIN > 8.0 was used.

RNA was converted to double-stranded cDNA and amplified using in vitro transcription with T7 polymerase. The in vitro transcription reaction included aminoallyl UTP (aa-dUTP), and the aa-dUTP nucleotides were later conjugated to Cy5 NHS ester (GE Healthcare Life Sciences, Pittsburg, PA). A quantity of 0.025 mg/mL fragmented Cy5-labeled cDNA was hybridized overnight at 42 °C using a HybBag mixing system with 1× OneArray Hybridization Buffer (Phalanx Biotech, San Diego, CA) and 0.01 mg/mL sheared salmon sperm DNA (Promega, Madison, WI). Following hybridization, the arrays were washed according to the OneArray protocol (Phalanx Biotech, San Diego, CA). A Molecular Devices Axon 4100A scanner was used to measure the raw Cy5 intensities produced by each of the microarrays. GenePix Pro software was used to measure the signals which were stored in GPR format.

2.3. Microarray data pre-processing and statistical analysis

Rosetta Resolver System® (Rosetta Biosoftware, USA) was used to analyze the data from all microarrays in each experimental set. Testing was performed in triplicate by combining technical replicates and performing statistical analyses using the proprietary modeling techniques of Rosetta Resolver [2]. The signal intensities were normalized using 75-percentile median centering. Average expression values were calculated using the error-weighted approach, which is specifically geared towards combining replicated hybridizations to improve measurement precision and accuracy. P-values were generated to test the null hypothesis that expression is absent (referred to as "P-value detected"), thereby providing an error-based statistical test for deciding whether a transcript is truly present. This test is especially important for determining whether genes with low average intensities are significantly above background. Lastly, P-values were calculated for calling genes differentially expressed. Rosetta Resolver does not calculate P-values based strictly on fold changes, but rather uses error-model-based hypothesis tests, which take into account fold change and expression level.

2.4. Microarray data quality control

Since three technical replicate hybridizations were performed and later averaged, care was taken to ensure high repeatability between technical replicates. First, raw and normalized $\log_2$ data for each sample were plotted using the R function *boxplot*. Control and flagged probes were not included. A representative box plot is shown in Fig. 1. While this analysis is designed to identify hybridizations that have intensity distributions different from those of their technical replicates, we did not find any instances of this. This analysis also ensures that the normalization has correctly centered the distributions of each replicate microarray.

Next, we compared scatter plots of raw and normalized $\log_2$ data for each sample using the R function *pairs*. Only data with a P-value detected <0.01 were included. A representative scatter plot is shown in Fig. 2. Scatter plots were viewed in conjunction with Pearson correlation tables. Correlation values were calculated from both raw and normalized $\log_2$ intensities for each technical repeat. Only probes with P-value detected <0.01 were included in the calculation. A representative correlation table is shown in Table 1. All correlation values were >0.961, and scatter plots confirmed high repeatability among technical replicates.

In our research article [1], we focused on differentially expressed genes underlying the different treatments described herein in our analysis of the transcriptomic data. Prior to this, we performed enrichment analyses using DAVID Bioinformatics [3] as a QC metric given

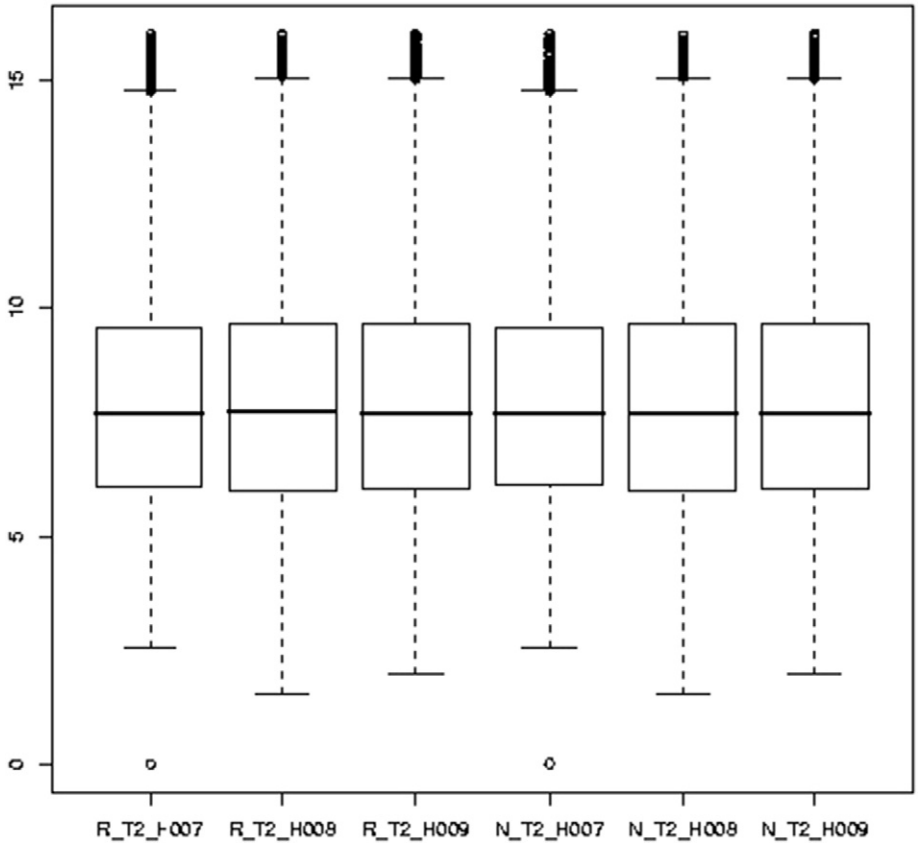

Fig. 1. Representative box plot of raw (R) and normalized (N) data from three technical replicate hybridizations of a single sample. For all samples, the box plots revealed median-centered raw data distributions, which were further refined during normalization. Overall, this points to high repeatability of technical replicate hybridizations.

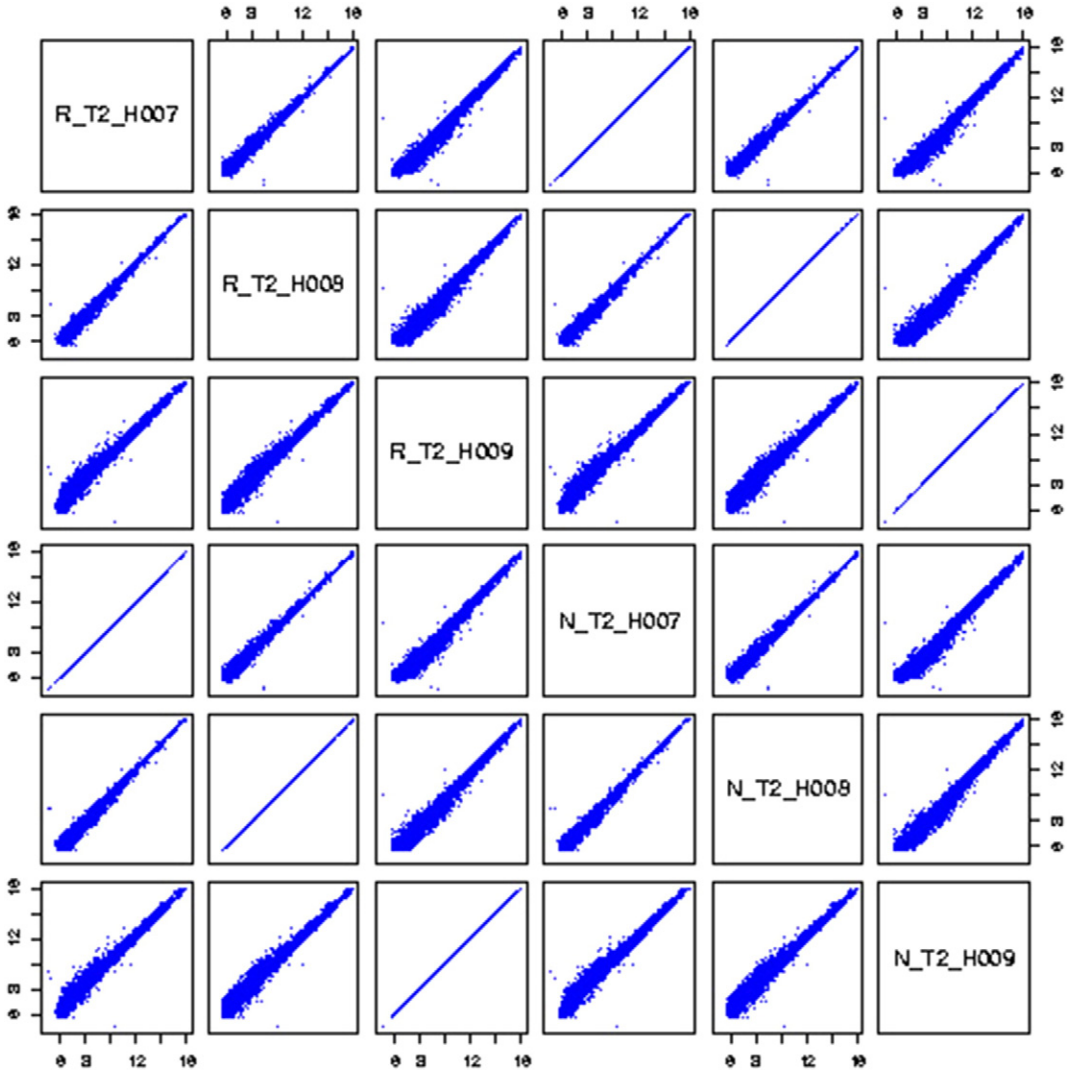

Fig. 2. Representative scatter plot of raw (R) and normalized (N) data from three technical replicate hybridizations of a single sample. For all samples, the scatter plots revealed tight correlation between raw and normalized data replicates, which overall, points to high repeatability of technical replicate hybridizations.

our expectations in irradiated and NAC–QYD treated samples. Up-regulated and down-regulated gene lists were analyzed separately in DAVID Bioinformatics. Genes with |fold change| > 1.5 and P-value < 0.05 were used. Gene symbols were used as input into DAVID Bioinformatics and default settings were used throughout. A Benjamini-adjusted P-value < 0.05 was used as a threshold for significance.

We hypothesized that non-treated, irradiated samples (compared to non-treated, non-irradiated control samples) would display patterns of gene expression consistent with the physiological effects of irradiation. Similarly, we hypothesized that irradiated samples pre-treated with NAC–QYD would display patterns of gene expression consistent with a protective effect of NAC–QYD. Table 2 lists the selected enriched categories from our QC enrichment analysis (Table S1 contains all enrichment analysis results). Indeed, we found enriched categories that were consistent with our hypotheses. For example, up-regulated genes in non-treated, irradiated samples were strongly enriched for mitochondrial respiration, which is a known response to irradiation that leads to oxidative stress [4–6]. Also, up-regulated genes in the NAC–QYD pre-treated, irradiated samples were strongly enriched for apoptosis. Notably, NAC–QYD treatment suppresses irradiation-induced apoptosis, so the enrichment results likely reflect anti-apoptotic mechanisms at work in

Table 1
Representative Pearson correlation table for raw (R) and normalized (N) data from three technical replicate hybridizations of a single sample.

	R_T2_H007	R_T2_H008	R_T2_H009	N_T2_H007	N_T2_H008	N_T2_H009
R_T2_H007	1	0.993	0.987	1	0.993	0.987
R_T2_H008	0.993	1	0.983	0.993	1	0.983
R_T2_H009	0.987	0.983	1	0.987	0.983	1
N_T2_H007	1	0.993	0.987	1	0.993	0.987
N_T2_H008	0.993	1	0.983	0.993	1	0.983
N_T2_H009	0.987	0.983	1	0.987	0.983	1

High correlation values were found for all replicate hybridizations for each sample, which indicate high repeatability among replicate hybridizations and minimal data transformation during normalization.

Table 2
Selected categories from an enrichment analysis using DAVID Bioinformatics.

Enriched term	Category	Count	Adj P-val
Up-regulated genes from non-treated, irradiated samples			
hsa00190:Oxidative phosphorylation	KEGG Pathway	21	1.21E−06
Respiratory chain	SP PIR Keyword	13	3.97E−04
GO:0005739~mitochondrion	GO CC	56	0.003
GO:0030964~NADH dehydrogenase complex	GO CC	8	0.007
GO:0030529~ribonucleoprotein complex	GO CC	29	0.037
Down-regulated genes from non-treated, irradiated samples			
Mutagenesis site	UniProt Seq Feature	124	2.35E−05
Serine/threonine–protein kinase	SP PIR Keyword	35	6.69E−05
GO:0005524~ATP binding	GO MF	99	8.38E−05
RNA-binding	SP PIR Keyword	43	1.32E−04
Chromatin regulator	SP PIR Keyword	20	0.010
ubl conjugation pathway	SP PIR Keyword	35	0.015
Transcription regulation	SP PIR Keyword	99	0.039
Protein transport	SP PIR Keyword	32	0.040
Up-regulated genes from NAC–QYD pre-treated, irradiated samples			
GO:0045449~regulation of transcription	GO BP	291	2.63E−07
GO:0042981~regulation of apoptosis	GO BP	100	0.002
GO:0001558~regulation of cell growth	GO BP	34	0.005
ubl conjugation	SP PIR Keyword	68	0.012
Down-regulated genes from NAC–QYD pre-treated, irradiated samples			
GO:0005739~mitochondrion	GO CC	144	2.79E−09
GO:0030529~ribonucleoprotein complex	GO CC	81	4.82E−08
GO:0034660~ncRNA metabolic process	GO BP	50	5.55E−08
GO:0045333~cellular respiration	GO BP	23	7.18E−04
GO:0006099~tricarboxylic acid cycle	GO BP	10	0.005
GO:0031396~regulation of protein ubiquitination	GO BP	20	0.024

The complete list of results, including the genes within each enriched term, can be found in Table S1. Both conditions (non-treated, irradiated and NAC–QYD pre-treated, irradiated) were compared to the non-treated, non-irradiated control samples. GO CC = Gene Ontology Cellular Component, MF = Molecular Function, and BP = Biological Process. Count = the number of differentially expressed genes annotated with a given enriched term. Adj P-val = Benjamini-adjusted P-values.

these samples. Overall, these results confirmed the quality of the microarray data and facilitated further interpretation of the data presented in Lambros et al. [1].

Conflict of interest

The authors declare that there are no competing interests.

Acknowledgments

We thank the ARDF Foundation for their generous support.

Appendix A. Supplementary data

Supplementary data to this article can be found online at http://dx.doi.org/10.1016/j.gdata.2015.07.029.

References

[1] M.P. Lambros, L. Kondapalli, C. Parsa, H.C. Mulamalla, R. Orlando, D. Pon, Y. Huang, M.S. Chow, Molecular signatures in the prevention of radiation damage by the synergistic effect of N-acetyl cysteine and qingre liyan decoction, a traditional Chinese medicine, using a 3-dimensional cell culture model of oral mucositis. Evid. Based Complement. Alternat. Med. 2015 (2015) 425760.
[2] L. Weng, H. Dai, Y. Zhan, Y. He, S.B. Stepaniants, D.E. Bassett, Rosetta error model for gene expression analysis. Bioinformatics 22 (9) (2006) 1111–1121.
[3] D.W. Huang, B.T. Sherman, R.A. Lempicki, Systematic and integrative analysis of large gene lists using DAVID bioinformatics resources. Nat. Protoc. 4 (1) (2009) 44–57.
[4] E.I. Azzam, J.P. Jay-Gerin, D. Pain, Ionizing radiation-induced metabolic oxidative stress and prolonged cell injury. Cancer Lett. 327 (1–2) (2012) 48–60.
[5] D. Candas, J.J. Li, MnSOD in oxidative stress response-potential regulation via mitochondrial protein influx. Antioxid. Redox Signal. 20 (10) (2014) 1599–1617.
[6] T. Yamamori, H. Yasui, M. Yamazumi, Y. Wada, Y. Nakamura, H. Nakamura, O. Inanami, Ionizing radiation induces mitochondrial reactive oxygen species production accompanied by upregulation of mitochondrial electron transport chain function and mitochondrial content under control of the cell cycle checkpoint. Free Radic. Biol. Med. 53 (2) (2012) 260–270.